processes

MDPI

Article

Dyes and Heavy Metals Removal from Aqueous Solutions Using Raw and Modified Diatomite

Simona Gabriela Muntean [1,*], Maria Andreea Nistor [1], Raisa Nastas [2] and Oleg Petuhov [2,3]

[1] "Coriolan Dragulescu" Institute of Chemistry, 24 Mihai Viteazul Str., 300223 Timisoara, Romania
[2] Institute of Chemistry, 3 Academiei Str., MD-2028 Chisinau, Moldova; petuhov.chem@gmail.com (O.P.)
[3] Research Centre for Thermal Analysis in Environmental Problems, West University of Timisoara, 16 Pestalozzi Street, 300115 Timisoara, Romania
* Correspondence: sgmuntean@acad-icht.tm.edu.ro

Abstract: The progress of the textile industry has led to a severe increase in the discharge of colored effluents, polluted with dyes and metal ions (non-biodegradable, carcinogenic to humans and environmental hazards). The implementation of effective methodologies and materials for the treatment of wastewater has become an urgent requirement. The present work describes the application of two samples of mineral materials—Ghidirim diatomite and modified diatomite—as adsorbents for the removal of dyes—Acid Blue 350, Methylene Blue, Basic Red 2—and of metal ions—copper, zinc, and lead—from aqueous solutions. In order to determine the optimal working conditions by which to ensure maximum removal efficiency, the influence of the nature and amount of the sorbent, the initial concentration of pollutant, and the temperature were studied. Working under normal conditions (room temperature, solution pH) efficiencies greater than 80% were obtained for the removal of dyes and metal ions. The adsorption fitted well with the pseudo-second order kinetic model, and the maximum adsorption capacities were determined from the Langmuir isotherm model. The adsorption of investigated pollutants is an endothermic and spontaneous process. The results indicate that Ghidirim diatomite and modified diatomite have potential applications in water purification management, providing high removal efficiency of both dyes and metal ions.

Keywords: wastewater; pollutant; adsorption; kinetic; equilibrium

Citation: Muntean, S.G.; Nistor, M.A.; Nastas, R.; Petuhov, O. Dyes and Heavy Metals Removal from Aqueous Solutions Using Raw and Modified Diatomite. *Processes* **2023**, *11*, 2245. https://doi.org/10.3390/pr11082245

Academic Editor: Maria Jose Martin de Vidales

Received: 3 July 2023
Revised: 22 July 2023
Accepted: 24 July 2023
Published: 26 July 2023

1. Introduction

Diatomite is a siliceous, sedimentary rock consisting predominantly of fossilized skeletal remains of diatoms, unicellular aquatic plants related to algae [1,2]. It is usually used for the manufacture of cement, clay diet, and bricks. From an economic point of view, the most promising and efficient use of these mineral resources is for the manufacture of adsorbents, filter powders, fillers and catalysts [3,4].

As a siliceous rock composed largely of diatoms, diatomite has a unique combination of physical and chemical properties that make it applicable as an adsorbent for the removal of heavy metals and organic pollutants from wastewater and as a filtration medium in several industrial uses [3,5–7]. Due to its high permeability and porosity, as well as its chemical inertness, many studies have addressed the application of diatomite as a low-cost adsorbent for dye and metal ion removal [8–11]. In the existing work, diatomite-based materials have been applied either for the removal of a dye (anionic or cationic) or metal ions, but never for both types of compounds. However, the use of diatomite for wastewater treatment is influenced by its origin and to increase its adsorption capacity, additional efforts must be made [8].

Releasing industrial effluents, often contaminated with dyes and metal ions, into the environment without proper treatment is one of the main causes of a series of health problems. In this context, ensuring the accessibility of clear water for different activities is

becoming a demanding task for researchers and engineers [12–15]. Research related to the treatment of colored wastewater has focused on obtaining new materials and applying appropriate and effective methods [16–18]. Undoubtedly, the enrichment of natural materials for the selective removal of ionic pollutants is a challenging research area.

Colored wastewater derives from industries such as dye manufacturing, textiles, wool spinning and others. Industrial dyes significantly change the aesthetic quality of water, affect photosynthesis by increasing the biochemical and chemical oxygen demands (BOD and COD, respectively), inhibit the growth of aquatic plants, enter the food chain and can have toxic, mutagenic and carcinogenic effects [19–21].

Although industrial dyes can cause allergic reactions in some people and hyperactivity in sensitive children, food dyes are found in processed, unhealthy foods [22].

Due to their toxicity and mobility in natural water ecosystems, metal ions have been reported as pollutants. The problem associated with metal ions pollution is that they are not biodegradable, cannot be metabolized or decomposed, and are highly persistent in the environment [23–25]. Examples of toxic metals are mercury, lead, arsenic, cadmium manganese, cobalt, copper, nickel, zinc, etc. The maximum permissible limit of heavy metals in drinking water according to the World Health Organization (WHO) and the potential health effects due to the toxicity of heavy metals are presented in Table 1 [26].

Table 1. Maximum permissible limit of investigated metals in drinking water and potential health effects.

Metal	The Maximum Limit Allowed by WHO (mg/L)	Potential Health Effects
Zinc	3–5	lethargy, anemia, dizziness, abdominal pain, vomiting, skin irritations
Cooper	1.5–2	kidney and liver damage; allergic contact dermatitis
Lead	0.05	affects kidney function, the nervous, immune, reproductive and the cardiovascular systems. Lead exposure also affects the oxygen carrying capacity of the blood.

The metal ions investigated (zinc, copper, lead) were selected taking into account the composition of a typical textile wastewater and based on data provided by the World Health Organization on metals of most immediate concern [26–29].

In the Republic of Moldova, considerable deposits of diatomite are localized along the course of the Dniester river. Nowadays, diatomite from these deposits is used exclusively in order to obtain construction materials. However, studies concerning other areas of Ghidirim diatomite application are performed. The application of chemical and physical treatments of diatomites modifies their surface properties and increases adsorption capacity.

Usually, natural diatomite contains impurity of the mineral and organic compounds that block the pores and diminish its absorption capacity. Therefore, it is necessary to remove the impurities from diatomite (pores) by chemical and/or thermal treatment [3–5,7–10]. For chemical treatment acid agents/activators (sulfuric acid, hydrochloric acid, phosphorous acid, etc.) or alkaline agents/activators (sodium hydroxide, sodium carbonate and potassium hydroxide) are used. Acid treatment reduces or eliminates all other oxides of diatomite relative to SiO_2, thus increasing its surface area and adsorption capacity. In this work sulfuric acid was used as activator.

The purpose of this study was to develop modified Ghidirim diatomite (Republic of Moldova) for environmental application. In order to remove dyes and heavy metal ions from solutions, two types of adsorbents were used: (i) mineral adsorbents—diatomite (D1) and modified diatomite with sulfuric acid (D2). The investigated materials are new and important for their abundance, cheapness and high surface area. Batch experiments were

conducted to evaluate the adsorption conditions for the removal of dyes and metal ions from aqueous solutions. Isotherm and kinetic studies were also performed.

2. Materials and Methods

2.1. Materials

The used diatomite sample was collected from Ghidirim village, Republic of Moldova. The collected diatomite was crushed and sieved. The fraction under 0.63 mm was washed with distilled water three times to remove any water-soluble contaminants. Then, the sample was dried in an oven at 110 °C and labeled as D1. The acid treatment was carried out with 3 M H_2SO_4 solution at a solid/liquid ratio of 1:25 (30 g diatomite/750 mL solution) in the water bath (90–95 °C) for 4 h in reflux conditions, and next the cooled suspension was filtered. The modified diatomite was washed with distilled water until a pH value of 7 was reached, then dried (110 °C) and calcined at 550 °C for 2 h. The obtained sample was labelled as D2.

One anionic (*Acid Blue 350*: AB, CAS 138067-74-0, $C_{28}H_{22}N_3NaO_7S_2$, Mw. 599.61) and two cationic (*Methylene Blue*: MB, C.I. 52015, $C_{16}H_{18}ClN_3S.3H_2O$, Mw. 373.90; *Basic Red 2*: RB2, C.I. 50240, $C_{20}H_{19}ClN_4$, Mw. 350.80) industrial dyes and three metal ions (Cu, Zn, Pb) were selected as potential pollutants.

Zinc chloride ($ZnCl_2$) and copper sulphate ($CuSO_4.5H_2O$) were purchased from Merck. Lead sulphate ($PbSO_4$) was obtained from Reactivul Bucuresti. HCl and NaOH solutions were used for pH adjustment.

2.2. Characterization of Materials

Bulk density value (g/cm^3) was determined according to the British standards for diatomite [30] and calculated using Equation (1):

$$Bulk\ density = \frac{m}{V} \quad (1)$$

where m (g) and V (mL) are the quantity and the volume of the sample, respectively.

Specific gravity value was calculated according to the British standards for diatomite [30], using Equation (2):

$$Specific\ gravity = \frac{B - A}{(B + D) - (A + C)} \quad (2)$$

where B is the mass of the pycnometer with 10 g of dry diatomite sample (g), A the mass of pycnometer (g), D the mass of pycnometer filled with distilled water (g), and C the mass of the pycnometer with 10 g of dry diatomite sample and filled with distilled water (g).

From the nitrogen adsorption isotherms performed at 77 K, the porous structure and adsorption parameters of the diatomite samples were determined. The adsorption isotherms were measured using Autosorb-1 (Quantachrome, Boynton Beach, FL, USA), after degassing the samples at 200 °C for 12 h. The density function theory (DFT) was used to calculate the pore size distribution.

The infrared spectra (IR) of the diatomite samples were recorded using a Fourier transform infrared spectrometer (PerkinElmer, Spectrum 100, Waltham, MA, USA), in the range 400–4000 cm^{-1}, applying the KBr pellet technique.

The pHpzc was determined based on the pH drift method [31,32]. Solutions of 0.01 mol/L NaCl with pHs between 2 and 12 were prepared by adding 0.1 or 1 mol/L HCl and 0.1 or 1 mol/L NaOH. Diatomite samples (D1, D2) were added to solutions with an appropriate pH value. After 24 h of stirring, the final pH of the solutions was measured. The pHpzc value was determined from the graph of ΔpH versus the initial pH.

2.3. Adsorption

The working solutions were prepared by diluting a volume of pollutant stock solution with distilled water so that the concentration of the pollutant in the working solution was within the studied concentration range. The adsorption experiments were carried out in

glass flasks containing pollutant solutions and diatomite samples (D1, D2), placed in a temperature-controlled shaker and stirred at a constant speed of 180 rpm [33,34]. The solution pH was adjusted to the desired values using HCl (0.1 mol/L) or NaOH (0.1 mol/L) solutions.

The concentration of dyes and metal ions in the solution was measured using a UV–Vis spectrophotometer and a SensAA atomic absorption spectrometer, respectively.

In order to evaluate the performance of the investigated materials as adsorbents, the percentage of pollutant removal (R) and the adsorption capacity (q_t) were calculated using equations:

$$R = \frac{(C_0 - C_e)\cdot 100}{C_0} \quad (3)$$

$$q_t = \frac{(C_0 - C_t)\cdot V}{w} \quad (4)$$

where C_0, C_t, and C_e are the pollutant concentration in solution at the initial time, time t, and at equilibrium time (mg/L), V is the volume of pollutant solution (L), and w is the quantity of adsorbent (g).

3. Results and Discussion

3.1. Characterization of Samples

Generally, depending on the mineralogical structure, diatomite can represent formations from well-crystallized forms (christobalite) to quite amorphous forms (opal). The mineral phase of the diatomite from Ghidirim in the Republic of Moldova contains several clay minerals, such as montmorillonite (in a mixture with insignificant quantities of slightly chlorinated montmorillonite), illite and kaolinite. Diatomite also contains non-clay components, such as finely dispersed quartz and amorphous material, the more probable sources of which are opal, amorphous alumosilicates, aluminums, and iron hydroxides [35].

The chemical composition of raw diatomite is silica (85.40%) and the remains include alumina (3.00%), iron oxide (1.90%), calcium oxide (1.80%) and magnesium oxide (0.60%).

Diatomite has a low specific gravity, in the range of 1.5–2.3 [8]. The specific gravity values were 0.38 and 0.35 g/cm^3 for D1 and D2 samples, and the bulk density was 2.02 and 1.99 for D1 and D2 samples, respectively.

The characteristics of the porous structure of the investigated samples are presented in Table 2. Analyzing the data, a 23% increase in the specific surface area was found for diatomite modified with sulfuric acid.

Table 2. Characteristics of porous structure of diatomite samples.

Sample	Total Pore Volume (cm^3/g)	Specific Surface Area (m^2/g)	Pore Width (nm)
D1	0.080	36	5.7
D2	0.087	47	2.4

Figure 1 presents the nitrogen adsorption–desorption isotherms on the initial diatomite samples (Figure 1a), and the diatomite modified with sulfuric acid (Figure 1a). It is observed that both isotherms have hysteresis, indicating the presence of mesopores in the porous structure of the samples. The same conclusion can be drawn from the pore distribution curves (Figure 1c,d). Activation with sulfuric acid leads to a decrease in the pore width from 5.7 nm to 2.4 nm, which leads to an increase in the specific surface area of the modified sample.

The FTIR spectra for the D1 and D2 samples were recorded and presented in Figure 2. The transmittance at 467–468 cm^{-1} is associated with the Si–O–H stretching vibration, and the strong peak at 1092–1094 cm^{-1} is attributed to Si–O stretching vibrations from Si–O–Si [4,24]. The absorption band at 803 cm^{-1} indicates the stretching vibration of O–H and also the Si–O–Si symmetric stretching vibrations. The FTIR band at 1634–1635 cm^{-1}

indicates the O–H bending vibration. The band at 3426–3428 cm^{-1} was associated with the stretching vibration of hydroxyl groups from Si–OH [27,36]. The obtained results confirm that silica was a component of the D1 and D2 materials.

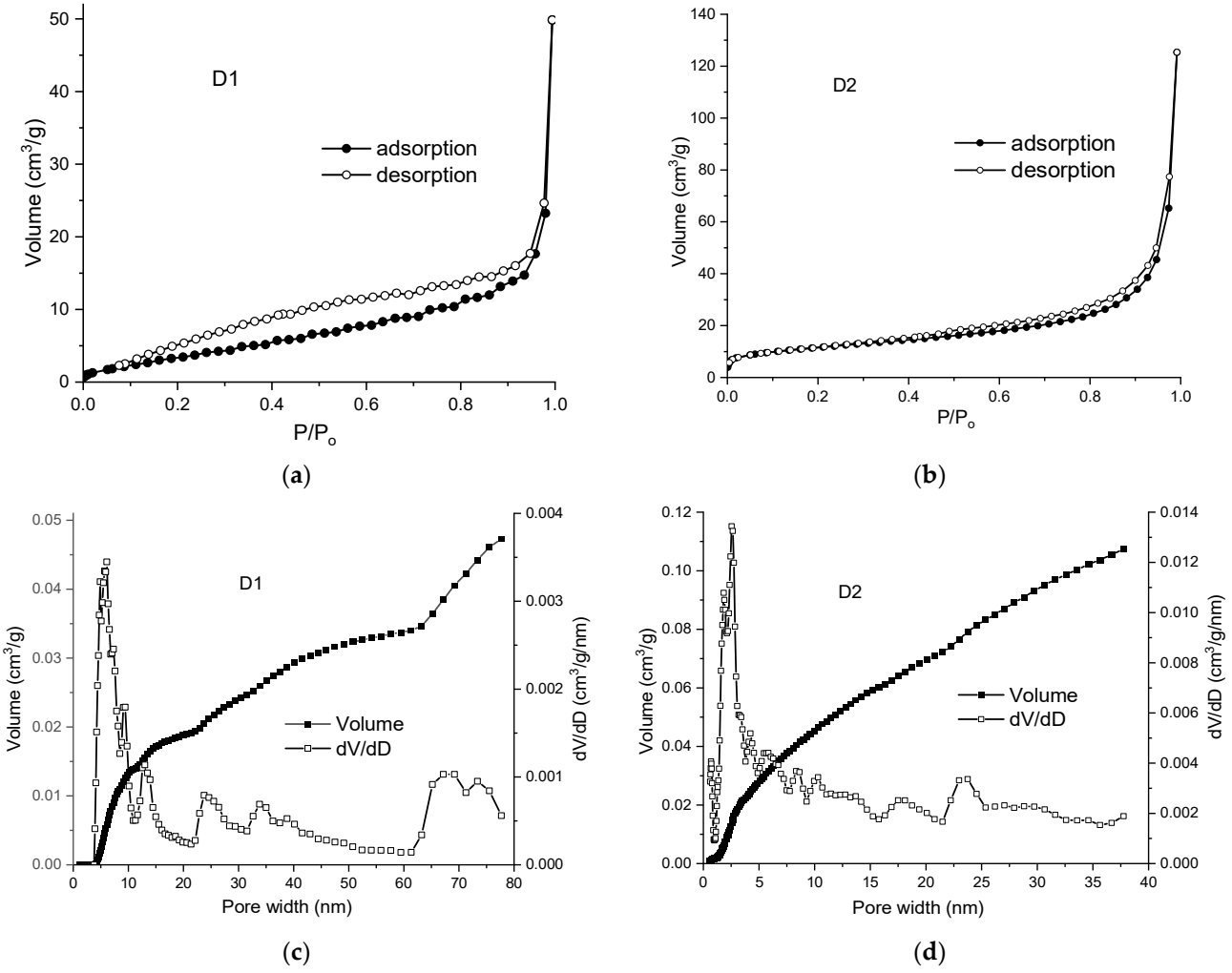

Figure 1. Nitrogen adsorption–desorption isotherms (**a**,**b**) and pore size distribution for (**c**) raw diatomite (D1) and (**d**) diatomite modified with H_2SO_4 (D2), obtained according to the DFT model.

The point of zero charge (pH_{PZC}) is a standard parameter that characterizes the surface charge of the material and defines the adsorption of ions [31,32]. The pHpzc of diatomite and modified diatomite were determined to be 6.4 and 4.6, respectively, as shown in Figure 3.

After sulfuric acid treatment the diatomite surface became more acidic, with a pronounced character as a cation exchanger. When the pH is lower than the pHpzc value, the surface of the adsorbent is positively charged (attracts anions). Conversely, above pHpzc the surface is negatively charged (attracting cations/repelling anions). The schematic representation of the protonation/deprotonation process of the adsorbent surface is presented in Supplementary File (Figure S2).

3.2. Adsorption Studies

3.2.1. Influence of the Adsorbent Nature

The porous diatomite samples (D1, D2) were applied as sorbents for the removal of one anionic (AB) and two cationic dyes (MB, RB2) and also for the removal of metal ions (Cu, Zn, Pb) from aqueous solutions. The study aims to investigate the adsorption capacities of the investigated materials, working in conditions as close as possible to

industrial working conditions. For this reason, the adsorption studies were carried out at room temperature (25 °C), the natural pH of the pollutant solution (7.2 AB, 6.9 MB, 6.7 RB2, 5.9 Cu(II), 5.8 Zn(II), 5.9 Pb(II)) with a concentration of 50 mg/L for dyes and 10 mg/L for metal ions, and a quantity of 1 g/L D1 and D2. The obtained results are presented in Figure 4.

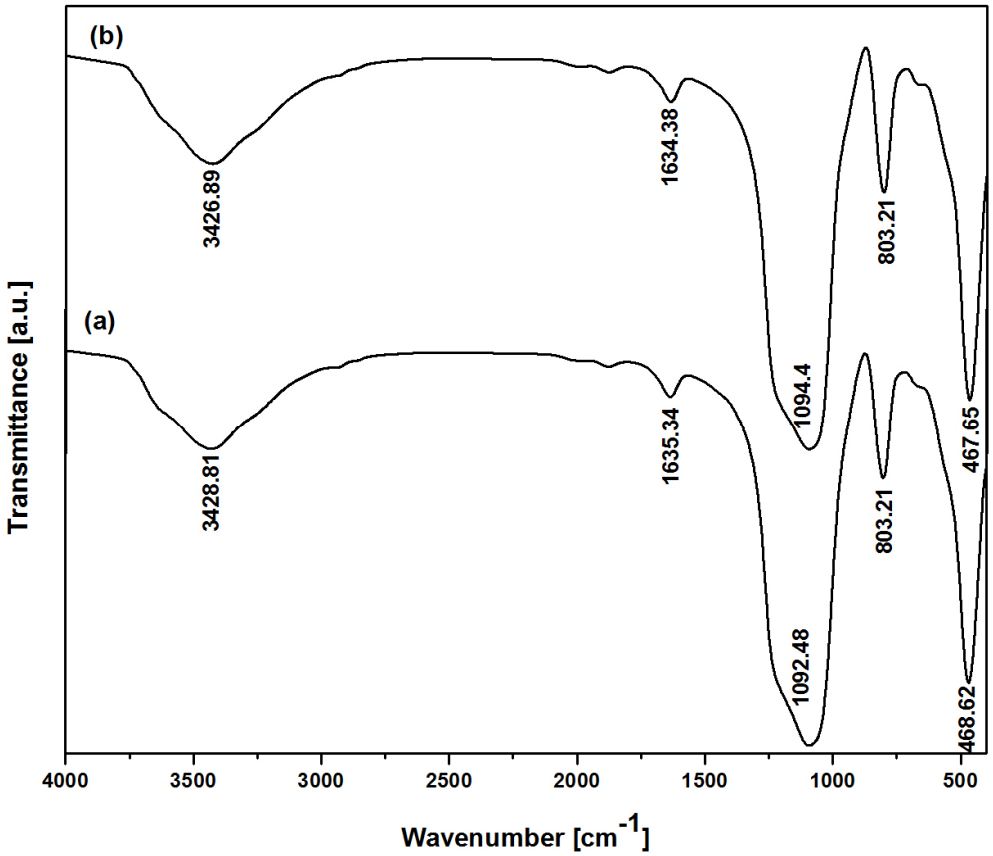

Figure 2. The FTIR spectra for D1 (a) and D2 (b) samples.

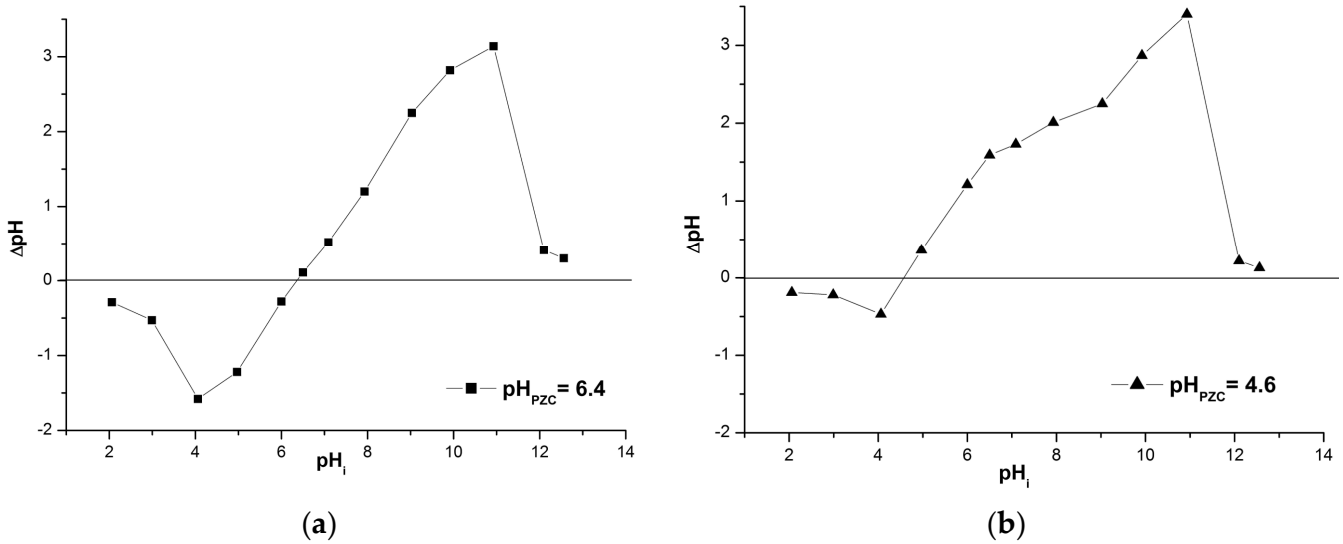

Figure 3. pH_{PZC} determination for (**a**) diatomite, and (**b**) modified diatomite with H_2SO_4.

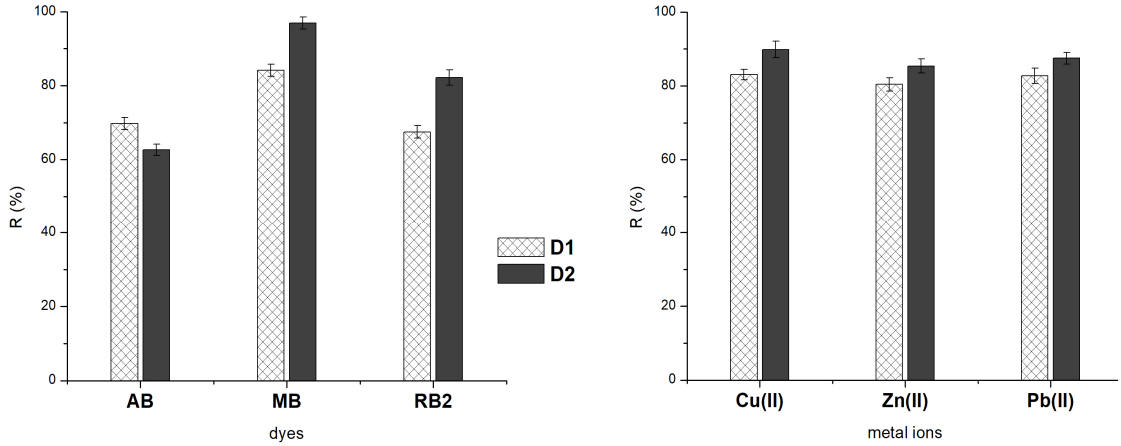

Figure 4. Effect of diatomite (D1) and modified diatomite (D2) on (**a**) dyes and (**b**) metal ions adsorption. (25 °C, pH: 7.2 AB, 6.9 MB, 6.7 RB2, 5.9 Cu(II), 5.8 Zn(II), 5.9 Pb(II), 50 mg/L dyes solution 10 mg/L metal ions solution, 1 g/L D1 and D2).

As can be seen, the removal efficiencies of positively charged species (cationic dyes and metal ions) are higher when the diatomite treated with acid (D2) was used as an adsorbent material. In the case of anionic dye AB, the removal efficiency is higher when diatomite (D1) was used as adsorbent. This behavior can be explained by the fact that, at a pH of 7.2, the surface charge of the D2 material is more negative than that of the D1, and thus electrostatic repulsions occur with the anionic dye. Using modified diatomite (D2) as adsorbent led to removal efficiencies of more than 85% for the removal of cationic species cationic dyes (MB, RB2) and metal ions (Cu, Zn, Pb). This is due to the electrostatic forces of attraction between the negatively charged surface of D2 and the positively charged pollutant molecules.

3.2.2. Influence of the Sorbent Quantity

The removal efficiency of the investigated dyes and the metal ions increases with increasing quantity of D1 and D2 (Figure 5). This result can be explained by the existence of an increased number of active centers on the surface of the adsorbent, along with the increase in the amount of material. Thus, the existence of a larger number of active centers ensures respectively higher adsorption capacities of D1 and D2, and therefore a higher pollutant removal efficiency [37–39].

Since the increase is less than 4% when the amount of adsorbent increases from 1 to 2 g/L, and considering the cost/effectiveness ratio, further studies were carried out using an amount of 1 g/L diatomite or modified diatomite. Additionally, as can be seen in Figure 5, removal efficiencies are higher when using D2 as an adsorbent material for positively charged pollutant molecules.

3.2.3. Effect of the Pollutant Initial Concentration

The initial concentration of the pollutant in the solution is another important factor for evaluating the adsorption capacity of a material applied as an adsorbent. In order to evaluate the influence of the initial concentration, studies were performed at room temperature (25 °C), the natural pH of the pollutant solution (7.2 AB, 6.9 MB, 6.7 RB2, 5.59 Cu(II), 5.8 Zn(II), 5.9 Pb(II)) and a quantity of 1 g/L D1 and D2. Dye and metal ion solutions with concentrations between 10 and 100 mg/L were investigated to study the impact of pollutant solution concentration on removal efficiency and adsorption capacity. The obtained results are presented in Figure 6.

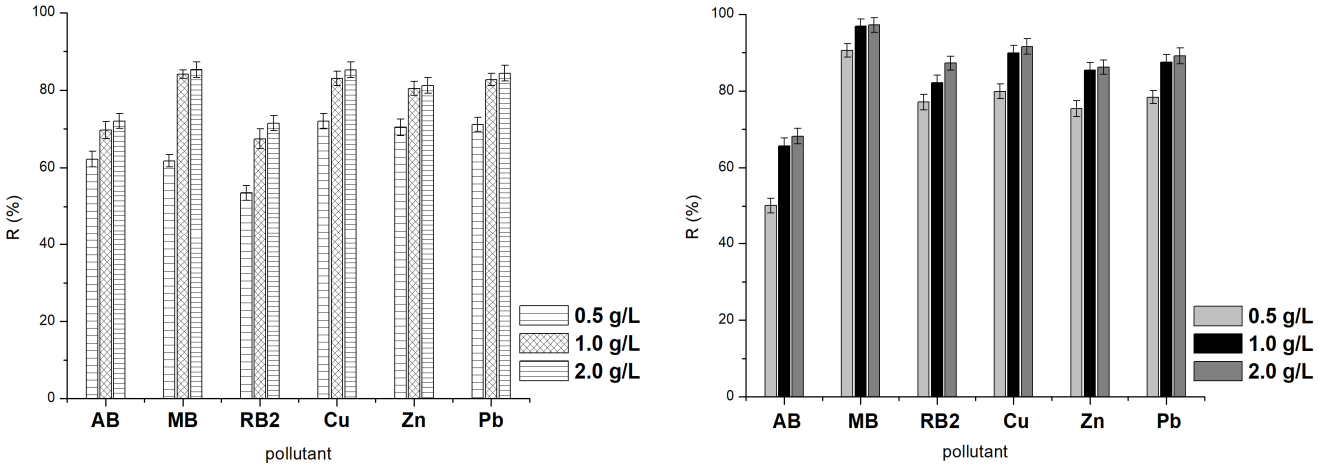

Figure 5. Effect of quantity of (**a**) diatomite (D1) and (**b**) modified diatomite (D2) on dyes and metal ions adsorption (25 °C, pH: 7.2 AB, 6.9 MB, 6.7 RB2, 5.9 Cu(II), 5.8 Zn(II), 5.9 Pb(II), 50 mg/L dyes solution 10 mg/L metal ions solution).

As can be seen in Figure 6 the adsorption capacity of both materials (D1, D2) increased and the removal efficiency decreased with increasing pollutant concentration in solution. The same behavior was highlighted in the literature using diatomite or modified diatomite [8,40,41] as adsorbents. An explanation of this behavior can be found in the fact that, with the increase in concentration, there are an increasing number of pollutant molecules per number of active centers on the surface of the adsorbent. As shown in Figure 6, the removal efficiency of pollutants from solution changes depending on the nature of the pollutant and also on the nature of the adsorbent. At low cationic pollutant concentrations (10 mg/L), yields greater than 80% were obtained using D2 as adsorbent and greater than 60% when D1 was used as adsorbent. In the case of anionic dye (AB) with increasing concentration in solution, the removal efficiency decreases from 80% to 62% using D2 as adsorbent and from 63% to 48% using D2 as adsorbent. The adsorption capacity of the investigated materials increases with the increase of the initial concentration of the pollutant in the solution [12,34].

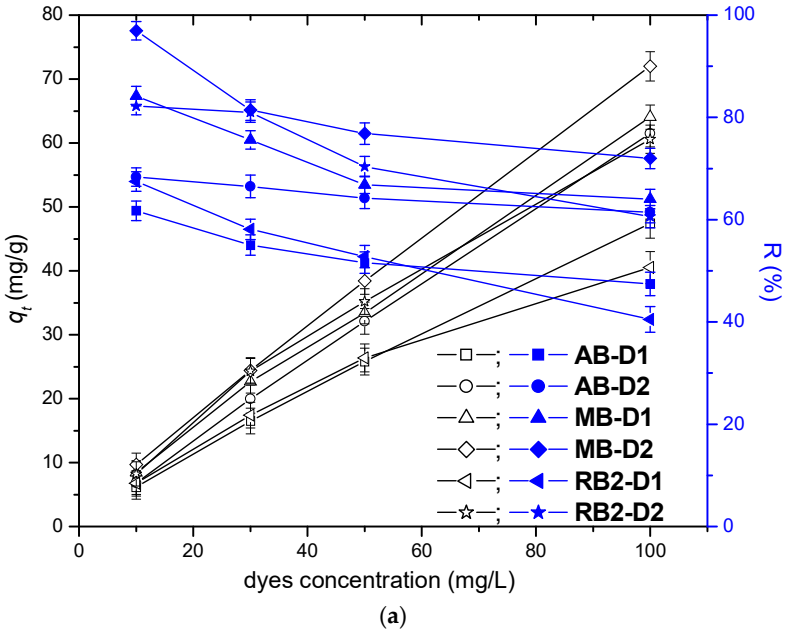

Figure 6. *Cont.*

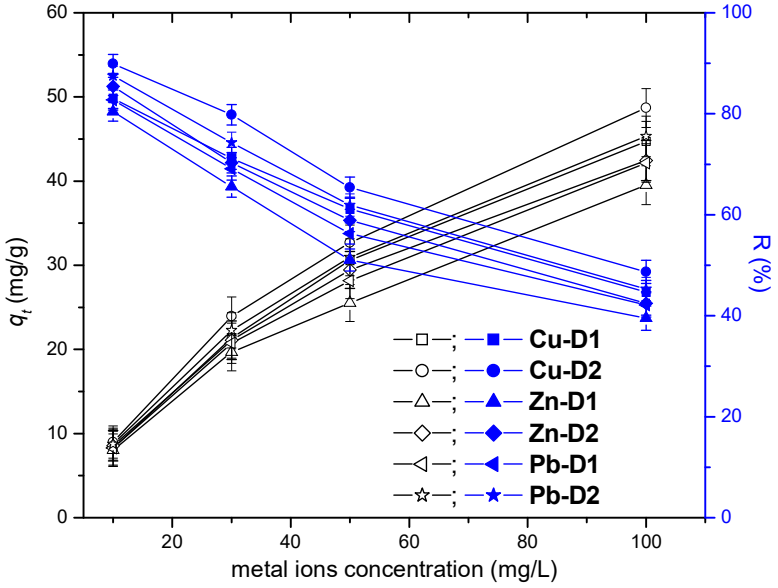

Figure 6. Influence of (**a**) dyes and (**b**) metal ions concentration on adsorption capacity (q_t) and removal efficiency (R) (25 °C, pH: 7.2 AB, 6.9 MB, 6.7 RB2, 5.9 Cu(II), 5.8 Zn(II), 5.9 Pb(II), 1 g/L D1 and D2).

3.2.4. Effect of the Temperature

The studies on the influence of temperature on the adsorption process were carried out at three temperatures of 25, 45 and 65 °C. As can be seen in Figure 7 for both tested materials and all investigated pollutants, their removal efficiency increases with increasing temperature, but the increase is less than 10%.

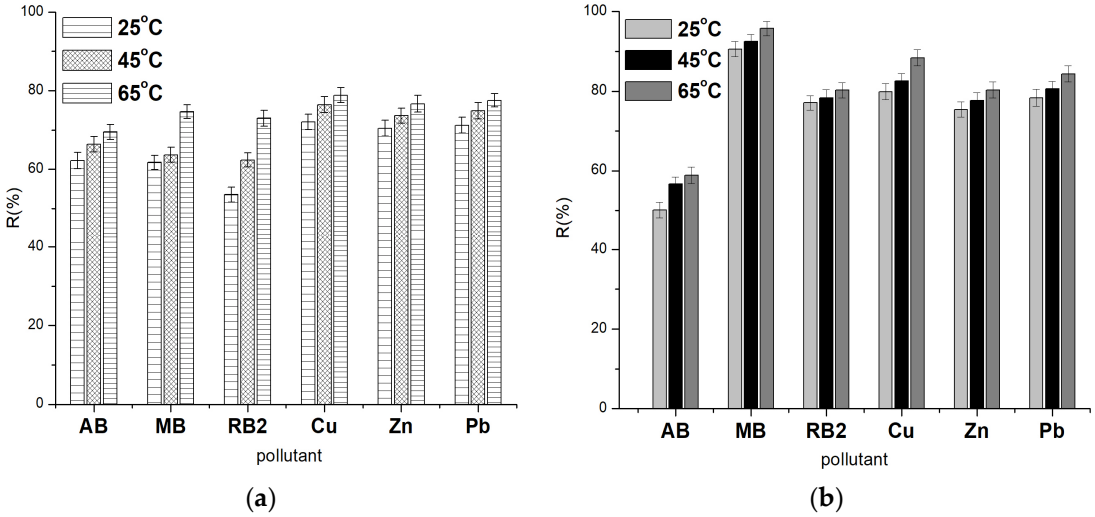

Figure 7. Influence of temperature on removal efficiency of pollutants using diatomite (**a**) and modified diatomite (**b**) as adsorbents (pH: 7.2 AB, 6.9 MB, 6.7 RB2, 5.9 Cu(II), 5.8 Zn(II), 5.9 Pb(II), 50 mg/L dyes solution 10 mg/L metal ions solution, 1 g/L D1 and D2).

By raising the temperature of the solution, the aggregation of dyes is diminished [42], the process of molecular transport of the dye is accelerated and the diffusion of dye molecules in the pores of the adsorbents is stimulated, which leads to an increase in the removal efficiency of the dyes [8]. The increase in adsorption efficiency with increasing temperature indicates the endothermic nature of the adsorption process. Similar results were obtained and are reported in the literature in regard to the use of diatomite and

modified diatomite as adsorbents [43–46]. Based on the results obtained, and taking into account the economic aspect, the adsorption studies were performed at room temperature.

3.3. Kinetic Studies

For the kinetic studies, 20 mg of adsorbent (D1, D2) were introduced into 20 mL of pollutant solutions of different concentrations at the natural pH of the solution and stirred at 25 °C for 240 min. At different time intervals, the absorbance was read and the concentration of the pollutants in the solution was determined. Experimental results were analyzed with pseudo first-order (5) [47] and pseudo second-order kinetic (6) equations [48]:

$$log(q_e - q_t) = logq_e - \frac{k_1}{2.303}t \quad (5)$$

$$\frac{t}{q_t} = \frac{1}{k_2 q_e^2} + \frac{1}{q_e}t \quad (6)$$

where q_t is the adsorption capacity at time t, q_e is the adsorption capacity at equilibrium, k_1 is the rate constant of pseudo first-order kinetic model (min^{-1}), k_2 is the rate constant for the pseudo second-order kinetic model (g/mg min).

Based on the higher values obtained for the correlation coefficients (R^2), and on the values of theoretical adsorption capacities close to the experimental ones (Tables 3 and 4), it was established that the pseudo second-order kinetic model best characterizes the adsorption process of the investigated pollutants from aqueous solutions, using D1 and D2.

Table 3. Parameters of the pseudo first- and pseudo second-order kinetic models for using D1 as adsorbent.

Pollutant	C_0 (mg/L)	$q_{e,exp}$ (mg/g)	Pseudo First-Order Kinetic Model				Pseudo Second-Order Kinetic Model			
			$q_{e,calc}$ (mg/g)	$k_1 \cdot 10^3$ (min^{-1})	R^2	SD	$q_{e,calc}$ (mg/g)	$k_2 \cdot 10^4$ (g/mg·min)	R^2	SD
AB	10	6.97	8.94	25.15	0.9815	0.1104	7.46	25.17	0.9861	1.1026
	30	19.86	30.67	10.64	0.9048	0.1102	21.39	2.53	0.9728	0.4309
	50	32.10	52.89	26.51	0.8751	0.1999	37.67	4.29	0.9317	0.7849
	100	61.47	101.89	21.44	0.8327	0.2678	95.01	0.74	0.8486	0.2873
MB	10	8.41	14.55	23.84	0.8233	0.3615	10.22	19.37	0.9913	0.7092
	30	21.55	40.24	26.51	0.8179	0.3483	29.98	4.59	0.9553	0.5453
	50	33.16	50.38	24.89	0.8509	0.1576	48.15	2.37	0.9267	0.4418
	100	64.04	132.46	28.19	0.7927	0.4015	113.12	0.59	0.8983	0.2249
RB2	10	6.40	7.73	15.52	0.9729	0.0847	6.59	29.67	0.9927	0.7852
	30	17.43	20.96	16.08	0.8941	0.1542	17.81	8.91	0.9799	0.1308
	50	26.38	34.99	21.58	0.9631	0.0839	32.09	4.32	0.9811	0.1484
	100	40.51	69.78	18.52	0.9307	0.1847	67.11	1.04	0.9422	0.2683
Cu(II)	10	8.30	6.42	26.22	0.9444	0.1976	8.64	9.22	0.9795	1.1643
	30	21.35	15.46	18.58	0.8577	0.1465	24.25	4.22	0.9845	1.0976
	50	30.58	54.24	27.11	0.7245	0.1987	37.45	2.66	0.9943	1.4064
	100	44.69	66.45	22.65	0.8456	0.1866	50.16	1.87	0.9766	1.0876
Zn(II)	10	8.04	15.51	18.44	0.9444	0.1875	11.25	20.44	0.9854	1.9431
	30	19.67	28.65	20.48	0.9254	0.2676	25.41	11.33	0.9866	1.1143
	50	25.52	32.64	22.52	0.8644	0.1632	30.52	6.44	0.9912	2.2876
	100	39.52	45.87	25,87	0.7866	0.1876	41.87	4.87	0.9765	1.9876
Pb(II)	10	8.27	20.45	26.36	0.9111	0.8232	14.52	9.57	0.9855	1.4340
	30	20.73	38.45	29.58	0.8755	0.1908	30.25	6.89	0.9914	2.1187
	50	28.15	49.81	18.55	0.8544	0.1254	31.42	2.21	0.9899	1.3982
	100	42.15	50.77	19.52	0.8654	0.1678	45.88	1.11	0.9815	1.2133

Table 4. Parameters of the pseudo first- and pseudo second-order kinetic models for using D2 as adsorbent.

Pollutant	C_0 (mg/L)	$q_{e,exp}$ (mg/g)	Pseudo First-Order Kinetic Model				Pseudo Second-Order Kinetic Model			
			$q_{e,calc}$ (mg/g)	$k_1 \cdot 10^3$ (min^{-1})	R^2	SD	$q_{e,calc}$ (mg/g)	$k_2 \cdot 10^4$ (g/mg·min)	R^2	SD
AB	10	6.57	7.36	15.41	0.8461	0.1453	6.43	24.13	0.9829	1.3821
	30	16.88	26.61	16.56	0.9322	0.0783	18.00	3.50	0.9665	0.6133
	50	27.21	39.03	15.41	0.9185	0.0849	31.62	1.96	0.9622	0.5165
	100	47.42	49.02	22.45	0.9214	0.1827	48.99	0.96	0.9833	0.1823
MB	10	9.69	68.19	0.49	0.7027	0.0117	10.79	31.90	0.9899	0.7221
	30	24.43	12.91	16.79	0.9230	0.1359	25.50	29.19	0.9989	0.0945
	50	38.43	45.71	16.93	0.8568	0.1926	39.27	4.45	0.9548	0.3626
	100	71.99	134.71	24.99	0.8879	0.24725	96.99	1.43	0.9834	0.3660
RB2	10	8.22	8.16	17.20	0.9568	0.1197	9.64	28.73	0.9879	0.7852
	30	24.31	28.65	23.58	0.9827	0.0872	28.38	9.39	0.9975	0.1308
	50	35.19	28.34	20.24	0.9631	0.1104	39.91	8.73	0.9939	0.1481
	100	60.58	69.95	20.70	0.7894	0.2978	67.78	3.39	0.9422	0.2683
Cu(II)	10	8.99	7.15	24.46	0.8462	0.7648	9.05	13.75	0.9915	2.2474
	30	23.94	42.46	14.58	0.8111	0.5864	29.41	10.56	0.9788	1.1587
	50	32.69	62.24	27.54	0.7844	0.4300	38.52	8.55	0.9854	1.4135
	100	42.69	71.45	26.76	0.8543	0.1876	46.98	6.88	0.9755	1.1643
Zn(II)	10	8.54	21.25	15.64	0.8954	0.8534	14.11	22.35	0.9955	3.1143
	30	21.09	34.25	1.88	0.8255	0.7643	27.21	15.64	0.9911	2.1554
	50	29.44	35.84	24.15	0.7888	0.5432	32.46	8.02	0.9855	1.2133
	100	42.44	55.65	19.66	0.7765	0.5014	44.33	6.22	0.9812	1.3971
Pb(II)	10	8.75	24.15	22.46	0.9142	0.8549	17.78	11.51	0.9945	2.0643
	30	22.28	40.25	24.58	0.8865	0.7876	33.52	9.65	0.9965	2.1199
	50	30.96	52.45	28.65	0.8145	0.4256	40.66	5.21	0.9845	1.1334
	100	45.32	61.87	26.44	0.7855	0.5672	48.66	3.66	0.9822	1.2131

With increasing pollutant concentration, the rate constant of the pseudo second-order kinetic model (k_2) decreases, indicating that the equilibrium time increases with increasing pollutant concentration. Similar results have been obtained by Medjdoubi [37], Sari [49], Yusan [50], and Tian [51], with regard to the use of diatomite or modified diatomite as adsorbents.

3.4. Equilibrium Studies

For the equilibrium studies, 2 g/L of adsorbent (D1, D2) were introduced into pollutant solutions of different concentrations (10, 30, 50, 100 and 200 mg/L) and stirred (250 rpm) at 25 °C in a thermostatic shaker until equilibrium was reached. The obtained experimental data (q_e and C_e) were analyzed with Freundlich (7) and Langmuir (8) adsorption isotherm models (Figure S3 Supplementary File):

$$q_e = K_F {C_e}^{1/n} \quad (7)$$

$$q_e = \frac{q_m K_L C_e}{1 + K_L C_e} \quad (8)$$

where *Ce* is the concentration at equilibrium of pollutant (mg/L), q_e is the adsorption capacity at equilibrium (mg/g), n exponent (dimensionless), K_F and K_L are the adsorption constants of Freundlich and Langmuir isotherm models, respectively.

The isotherm parameters were determined by non-linear regression analysis [52] and are presented in Table 5. Based on the obtained values of the correlation coefficients (R^2

and Chi^2), the Langmuir was determined to be the best model to fit the experimental data (Table 5).

Table 5. Parameters of Freundlich and Langmuir isotherms.

Pollutant	Adsorbent	Freundlich				Langmuir			
		K_F (mg/g(mg/L)$^{1/n}$)	n	R^2	Chi^2	q_m (mg/g)	K_L (L/mg)	R^2	Chi^2
AB	D1	5.68	1.64	0.9769	38.42	152.66	0.016	0.9967	5.50
	D2	4.69	1.85	0.9638	26.90	92.76	0.018	0.9935	4.85
MB	D1	9.69	2.09	0.9644	50.27	116.51	0.030	0.9871	18.20
	D2	12.68	2.06	0.9843	34.71	148.95	0.031	0.9885	25.34
RB2	D1	4.75	1.92	0.9909	5.46	81.67	0.019	0.9931	4.16
	D2	8.95	1.94	0.9797	32.75	131.33	0.026	0.9955	7.35
Cu(II)	D1	11.03	3.14	0.9445	22.27	55.86	0.07	0.9945	2.19
	D2	13.63	3.36	0.9612	18.74	58.87	0.0949	0.9734	12.82
Zn(II)	D1	9.16	3.09	0.9512	14.19	49.13	0.05	0.9732	7.79
	D2	11.03	3.26	0.9564	14.98	52.15	0.0735	0.9841	5.48
Pb(II)	D1	9.91	3.02	0.9638	13.04	53.92	0.06	0.9825	6.28
	D2	11.79	3.18	0.9692	13.18	57.09	0.0754	0.9799	8.57

The obtained results indicate that the surface of the adsorbents are homogeneous, and adsorption takes place on well-defined specific sites. The pollutant is adsorbed in a monomolecular layer on the surface of the adsorbent and therefore there is a limit of adsorption. The maximum adsorption capacities of the D1 and D2 were determined from the Langmuir isotherm curves, and the results are presented in Table 5.

To assess the capacity of diatomite and modified diatomite to remove dyes and metal ions from aqueous solutions, the obtained adsorption capacities were compared with other results reported in the literature for diatomite-based adsorbents (Table 6). As can be seen, the values obtained in this work are comparable to or higher than other reported data.

Table 6. The maximum adsorption capacities obtained when using diatomite or modified diatomite as adsorbents.

Pollutant	Adsorbent	q_t (mg/g)	Reference
Orange Bezaktiv (SRL-150)	diatomite	14.23	[10]
Janus Green B	Algerian diatomite	39.89	[37]
Rhodamine-B	diatomite	10.21	[46]
Sıf Blau BRF Everzol Brill Red 3BS Int Yellow 5GF	diatomite earth samples	10.11 5.92 117.75	[53]
Methylene Blue	diatomite	72	[38]
	modified diatomite	127	
	diatomite	66.7	[4]
	diatomite	47.7	[54]
	$Mg(OH)_2$-modified diatomite	41.5	
Ramazol Golden Yellow	diatomite	8.06	
	$Mg(OH)_2$-modified diatomite	53.70	
Telon Blue	diatomite	109.00	
	$Mg(OH)_2$-modified diatomite	173.90	

Table 6. *Cont.*

Pollutant	Adsorbent	q_t (mg/g)	Reference
Acid Blue 350	diatomite modified diatomite	152.66 92.76	Present paper
Methylene Blue	diatomite modified diatomite	116.51 148.95	
Basic Red 2	diatomite modified diatomite	81.67 131.33	
Cd(II)	novel diatom-based Cd(II) ion-imprinted polymer	5.502	[45]
Co(II)	modified diatomaceous ceramic	31.29	[55]
Pb(II)	diatomite	56.49	[43]
	diatomite	66.28	[56]
	diatomite	26.00	[57]
Cu(II)	modified diatomaceous ceramic Punice	121.80 1.43	[55] [36]
Cr(II)	Mag-GO-diatomite diatomite	0.0622 167.00	[58] [4]
Cu(II) Pb(II)	Mag-GO-diatomite	0.0268 113.50	[58]
Cu(II) Cd(II) Zn(II)	modified diatomite	11.40 5.41 7.22	[59]
Cu(II)	diatomite modified diatomite	55.86 58.87	Present paper
Pb(II)	diatomite modified diatomite	49.13 52.15	
Zn(II)	diatomite modified diatomite	53.92 57.09	

3.5. Thermodynamic Parameters

The free energy change ΔG was calculated from Equation (9), using the obtained Langmuir constants, at different temperatures: 298, 318 and 338 K, and the results are presented in Table 7. The standard entropy and standard enthalpy were obtained (Table 7) from the slope and intercept of the plot lnK_L versus 1/T (Equation (10)):

$$\Delta G^0 = -RTlnK \tag{9}$$

$$lnK = \frac{\Delta S^0}{R} - \frac{\Delta H^0}{RT} \tag{10}$$

where R is the general gas constant (8.314 J/mol·K), T is the absolute temperature (K) and K_L is the adsorption Langmuir constant.

The values of ΔG were negative for all three temperatures, and for all investigated pollutants, indicating that the adsorption was a spontaneous process. The ΔG values decrease with increasing temperature indicating that high temperature is conducive to adsorption. The obtained values of ΔH were positive, indicating the endothermic nature of the adsorption of investigated dyes and metal ions onto modified diatomite (D2). Additionally, the ΔH values less than 40 kJ/mol indicated that the process is a physical adsorption. The positive values of ΔS indicate the affinity of the modified diatomite for the investigated dyes and metal ions due to the increased randomness at the interface between the solid–liquid phases [7,60,61].

Table 7. Thermodynamic parameters for adsorption of investigated pollutants onto modified diatomite.

Pollutant	Temperature (K)	ΔG^0 (kJ/mol)	ΔH^0 (kJ/mol)	ΔS^0 (J/mol·K)
AB	298	−15.53	6.66	74.51
	318	−17.05		
	338	−18.53		
MB	298	−15.48	12.13	92.08
	318	−16.73		
	338	−19.26		
RB2	298	−14.65	17.52	107.73
	318	−16.58		
	338	−19.01		
Cu(II)	298	−18.36	7.71	87.55
	318	−20.18		
	338	−21.86		
Zn(II)	298	−18.18	6.41	82.53
	318	−19.79		
	338	−21.50		
Pb(II)	298	−18.24	7.07	84.96
	318	−19.96		
	338	−21.63		

4. Conclusions

In this work, Ghidirim diatomite (Republic of Moldova) and modified diatomite with sulfuric acid were used as adsorbents for the removal of dyes (Acid Blue 350, Methylene Blue, Basic Red 2) and metal ions (Cu(II), Zn(II), Pb(II)) from aqueous solutions. The physicochemical peculiarities of the diatomite samples were evaluated by nitrogen sorption–desorption isotherms, bulk density and specific gravity, IR spectra and pHpzc. According to obtained results, the treatment of diatomite with sulfuric acid led to an increase in specific surface area (with 23%), at the same time, the surface acquired a more acidic character.

High removal efficiencies were obtained when working in normal conditions (natural solution pH, room temperature), and the values increased with increasing quantity of adsorbent, temperature, and decreased with increasing initial pollutant concentration. The results indicate that the adsorption fitted well with the pseudo second-order kinetic model. The maximum adsorption capacities were determined from the Langmuir isotherm model, our obtained results are higher than or comparable to published data. Thermodynamic parameters show that the adsorption of Acid Blue 350, Methylene Blue, Basic Red 2 Cu(II), Zn(II), and Pb(II) onto the modified diatomite is an endothermic and spontaneous process.

The obtained results indicate that both investigated materials have potential applications in water purification management, but higher efficiencies were obtained using modified diatomite as adsorbent.

Supplementary Materials: The following supporting information can be downloaded at: https://www.mdpi.com/article/10.3390/pr11082245/s1, Figure S1: X-ray diffractograms of the Ghidirim diatomite. Non-calcinated samples (A), after calcinations at 350 °C (B) and 550 °C (C); Figure S2: Schematic representation of the protonation/deprotonation process of the adsorbent surface; Figure S3: Isotherms adsorption plots for the adsorption of: (a) dyes on D1, (b) dyes on D2, (c) metal ions on D1, (d) metal ions on D2. (See Refs. [35,62]).

Author Contributions: Conceptualization, S.G.M.; methodology, S.G.M. and O.P.; validation, S.G.M. and R.N.; formal analysis, O.P.; investigation, M.A.N.; writing—original draft preparation, S.G.M. and M.A.N.; writing—review and editing, S.G.M.; visualization, R.N.; supervision, S.G.M. All authors have read and agreed to the published version of the manuscript.

Funding: This research received no external funding.

Data Availability Statement: Not applicable.

Acknowledgments: This work was supported by Program 2 of the "Coriolan Dragulescu" Institute of Chemistry (Research Project 2.3.) and by Moldova State Program, project DISTOX, no. NARD/20.80009.7007.21. Authors would like to thank Adelina Andelescu from "Coriolan Drăgulescu" Institute of Chemistry, for atomic absorption spectroscopy measurements.

Conflicts of Interest: The authors declare no conflict of interest.

References

1. Flower, R.J. Diatomites: Their Formation, Distribution, and Uses. Diatom methods. In *Encyclopedia of Quaternary Science*, 2nd ed.; Scott, A.E., Cary, J.M., Eds.; Elsevier: Amsterdam, The Netherlands, 2013; pp. 501–506. [CrossRef]
2. Cameron, N.G.; Diatoms Scott, A.E.; Cary, J.M. (Eds.) *Encyclopedia of Quaternary Science*, 2nd ed.; Elsevier: Amsterdam, The Netherlands, 2013; pp. 522–525, ISBN 9780444536426.
3. Ghobara, M.M.; Ghobara, M.M.; Ghobara, M.M.; Mohamed, A. Diatomite in use: Nature, modifications, commercial applications and prospective trends. In *Diatoms: Fundamentals and Applications*; Seckbach, J., Gordon, R., Eds.; Scrivener Publishing LLC: Beverly, MA, USA, 2019; pp. 471–509.
4. Fathy, N.A.; Mousa, S.M.; Aboelenin, R.M.; Sherief, M.A.; Abdelmoaty, A.S. Strengthening the surface and adsorption properties of diatomite for removal of Cr(VI) and methylene blue dye. *Arab. J. Geosci.* **2022**, *15*, 1664–1675. [CrossRef]
5. Datsko, T.I.; Zelentsov, V.I. Effect of microstructure of modified diatomite on its adsorption properties. *Chem. Phys. Technol. Surf.* **2017**, *8*, 65–72.
6. Tzvetkova, P.G.; Nickolov, R.N.; Tzvetkova, C.T.; Bozhkov, O.D.; Voykova, D.K. Diatomite/carbon adsorbent for phenol removal. *J. Chem. Technol. Metall.* **2016**, *51*, 202–209.
7. Yang, X.; Zhang, Y.; Wang, L.; Cao, L.; Li, K.; Hursthouse, A. Preparation of a thermally modified diatomite and a removal mechanism for 1-naphthol from solution. *Water* **2017**, *9*, 651. [CrossRef]
8. Sriram, G.; Kigga, M.; Uthappa, U.T.; Rego, R.M.; Thendral, V.; Kumeria, T.; Jung, H.Y.; Kurkuri, M.D. Naturally available diatomite and their surface modification for the removal of hazardous dye and metal ions: A review. *Adv. Colloid Interface Sci.* **2020**, *282*, 102198. [CrossRef]
9. Sogut, E.G.; Caliskan, N. Removal of lead, copper and cadmium ions from aqueous solution using raw and thermally modified diatomite. *Desalination Water Treat.* **2017**, *58*, 154–167. [CrossRef]
10. Aguedal, H.; Iddou, A.; Aziz, A.; Merouani, D.R.; Bensaleh, F.; Bensadek, S. Removal of textile dye from industrial wastewater by natural and modified diatomite. *WASET J. Fash. Technol. Text. Eng.* **2016**, *10*, 1317–1320.
11. Badawi, A.K.; Elkodous, M.A.; Ali, G.A.M. Recent advances in dye and metal ion removal using efficient adsorbents and novel nano-based materials: An overview. *RSC Adv.* **2021**, *11*, 36528–36553. [CrossRef]
12. Muntean, S.G.; Todea, A.; Bakardjieva, S.; Bologa, C. Removal of non benzidine direct red dye from aqueous solution by using natural sorbents: Beech and silver fir. *Desalination Water Treat.* **2017**, *66*, 235–250. [CrossRef]
13. Rathi, B.S.; Kumar, P.S.; Vo, D.V.N. Critical review on hazardous pollutants in water environment: Occurrence, monitoring, fate, removal technologies and risk assessment. *Sci. Total Environ.* **2021**, *797*, 149134. [CrossRef]
14. WWAP (United Nations World Water Assessment Programme). *The United Nations World Water Development Report 2015: Water for a Sustainable World*; United Nations World Water Assessment Programme: Paris, France, 2015; ISBN 978-92-3-100071-3.
15. National Research Council, Division on Earth and Life Studies, Commission on Geosciences, Environment and Resources, Committee. *Review the New York City Watershed Management Strategy Watershed Management for Potable Water Supply: Assessing the New York City Strategy*; National Academies Press: Washington, DC, USA, 2000; ISBN 0309067774/9780309067775.
16. Alqadami, A.A.; Khan, M.A.; Otero, M.; Siddiqui, M.R.; Jeon, B.-H.; Batoo, K.M. A magnetic nanocomposite produced from camel bones for an efficient adsorption of toxic metals from water. *J. Clean. Prod.* **2018**, *178*, 293–304. [CrossRef]
17. Saleh, T.S.; Badawi, A.K.; Salama, R.S.; Mostafa, M.M.M. Design and development of novel composites containing nickel ferrites supported on activated carbon derived from agricultural wastes and its application in water remediation. *Materials* **2023**, *16*, 2170. [CrossRef] [PubMed]
18. Dutta, S.; Gupta, B.; Srivastava, S.K.; Gupta, A.K. Recent advances on the removal of dyes from wastewater using various adsorbents: A critical review. *Mater. Adv.* **2021**, *2*, 4497–4531. [CrossRef]
19. Lellis, B.; Fávaro-Polonio, C.Z.; Pamphile, J.A.; Polonio, J.C. Effects of textile dyes on health and the environment and bioremediation potential of living organisms. *Biotechnol. Res. Innov.* **2019**, *3*, 275–290. [CrossRef]
20. Berradi, M.; Hsissou, R.; Khudhair, M.; Assouag, M.; Cherkaoui, O.; El Bachiri, A.; El Harfi, A. Textile finishing dyes and their impact on aquatic environs. *Heliyon* **2019**, *5*, e02711. [CrossRef]
21. Hadia-e-Fatima, A.A. Heavy metal pollution—A mini review. *J. Bacteriol. Mycol. Open Access.* **2018**, *6*, 179–181.
22. Dey, S.; Nagababu, B.H. Applications of food color and bio-preservatives in the food and its effect on the human health. *Food Chem. Adv.* **2022**, *1*, 100019. [CrossRef]

23. Briffa, J.; Sinagra, E.; Blundell, R. Heavy metal pollution in the environment and their toxicological effects on humans. *Heliyon* **2020**, *6*, e04691. [CrossRef] [PubMed]
24. Qasem, N.A.A.; Mohammed, R.H.; Lawal, D.U. Removal of heavy metal ions from wastewater: A comprehensive and critical review. *NPJ Clean Water* **2021**, *4*, 36. [CrossRef]
25. Shubair, T.; Tahara, A.; Khandaker, S. Optimizing the magnetic separation of strontium ion using modified zeolite with nano iron particles. *Case Stud. Chem. Environ. Eng.* **2022**, *6*, 100243–100253. [CrossRef]
26. Braga, M.; Jaimes, R.; Borysow, W.; Gomes, O.; Salcedo, W. Portable multispectral colorimeter for metallic ion detection and classification. *Sensors* **2017**, *17*, 1730. [CrossRef]
27. Jawad, A.H.; Abdulhameed, A.S.; Kashi, E.; Yaseen, Z.M.; ALOthman, Z.A.; Khan, M.R. Cross-Linked chitosan-glyoxal/kaolin clay composite: Parametric optimization for color removal and COD reduction of Remazol Brilliant Blue dye. *J. Polym. Environ.* **2021**, *30*, 164–178. [CrossRef]
28. Hussein, F.H. Chemical properties of treated textile dyeing wastewater. *Asian J. Chem.* **2013**, *25*, 9393–9400. [CrossRef]
29. Yaseen, D.A.; Scholz, M. Textile dye wastewater characteristics and constituents of synthetic effluents: A critical review. *Int. J. Environ. Sci. Technol.* **2018**, *16*, 1193–1226. [CrossRef]
30. Inglethorpe, S.D.J. Industrial Minerals Laboratory Manual. In *Diatomite*; Technical report WG/92/39; Mineralogy and Petrology Series; British Geological Survey: Nottingham, UK, 1992.
31. Al-Maliky, E.A.; Gzar, H.A.; Al-Azawy, M.G. Determination of point of zero charge (PZC) of concrete particles adsorbents. *IOP Conf. Ser. Mater. Sci. Eng.* **2021**, *1184*, 012004. [CrossRef]
32. Nasiruddin Khan, M.; Sarwar, A. Determination of points of zero charge of natural and treated adsorbents. *Surf. Rev. Lett.* **2007**, *14*, 461–469. [CrossRef]
33. Muntean, S.G.; Nistor, M.A.; Ianoș, R.; Păcurariu, C.; Căpraru, A.; Surdu, V.-A. Combustion synthesis of Fe_3O_4/Ag/C nanocomposite and application for dyes removal from multicomponent systems. *Appl. Surf. Sci.* **2019**, *481*, 825–837. [CrossRef]
34. Andelescu, A.; Nistor, M.A.; Muntean, S.G.; Rădulescu-Grad, M.E. Adsorption studies on copper, cadmium, and zinc ion removal from aqueous solution using magnetite/carbon nanocomposites. *Sep. Sci. Technol.* **2018**, *53*, 2352–2364. [CrossRef]
35. Rusu, V.; Vrânceanu, A.; Polevoi, I. Composition of mineral phases of the Ghidirim diatomite. *Chem. J. Mold.* **2007**, *2*, 63–66. [CrossRef] [PubMed]
36. Öztürk, D.; Şahan, T. Design and optimization of Cu(II) adsorption conditions from aqueous solutions by low-cost adsorbent pumice with Response Surface Methodology. *Pol. J. Environ. Stud.* **2015**, *24*, 1749–1756. [CrossRef]
37. Medjdoubi, Z.; Hachemaoui, M.; Boukoussa, B.; Hakiki, A.; Bengueddach, A.; Hamacha, R. Adsorption behavior of Janus Green B dye on Algerian diatomite. *Mater. Res. Express* **2019**, *6*, 085544. [CrossRef]
38. Ebrahimi, P.; Kumar, A. Diatomite chemical activation for effective adsorption of methylene blue dye from model textile wastewater. *Int. J. Environ. Sci. Dev.* **2021**, *12*, 23–28. [CrossRef]
39. El Sayed, E.E. Natural diatomite as an effective adsorbent for heavy metals in water and wastewater treatment (a batch study). *Water Sci.* **2018**, *32*, 32–43. [CrossRef]
40. Kubilay, Ş.; Gürkan, R.; Savran, A.; Sahan, T. Removal of Cu(II), Zn(II) and Co(II) ions from aqueous solutions by adsorption onto natural bentonite. *Adsorption* **2007**, *13*, 41–51. [CrossRef]
41. Akafu, T.; Chimdi, A.; Gomoro, K. Removal of Fluoride from drinking water by sorption using diatomite modified with aluminum hydroxide. *J. Anal. Chem.* **2019**, *2019*, 4831926. [CrossRef]
42. Muntean, S.G.; Simu, G.M.; Kurunczi, L.; Szabadai, Z. Investigation of the aggregation of three disazo direct dyes by UV-Vis spectroscopy and mathematical analysis. *Rev. Chim.* **2009**, *60*, 152–155.
43. Bilgin, M.; Tulun, Ş. Use of diatomite for the removal of lead ions from water: Thermodynamics and kinetics. *Biotechnol. Biotechnol. Equip.* **2015**, *29*, 696–704. [CrossRef]
44. Flores-Cano, J.V.; Leyva-Ramos, R.; Padilla-Ortega, E.; Mendoza-Barron, J. Adsorption of heavy metals on diatomite: Mechanism and effect of operating variables. *Adsorp. Sci. Technol.* **2013**, *31*, 275–291. [CrossRef]
45. Huang, L.; Wang, L.; Gong, L.; Xie, Q.; Chen, N. Preparation, characterization and adsorption characteristics of diatom-based Cd(II) surface ion-imprinted polymer. *J. Dispers. Sci. Technol.* **2022**, *43*, 1321–1332. [CrossRef]
46. Koyuncu, M.; Kul, A.R. Thermodynamics and adsorption studies of dye (rhodamine-b) onto natural diatomite. *Physicochem. Probl. Miner. Process.* **2014**, *50*, 631–643.
47. Lagergreen, S. About the theory of so-called adsorption of soluble substances. *Vetenskapsakad Handl.* **1898**, *24*, 1–39.
48. Ho, Y.S.; McKay, G. Pseudo-second order model for sorption processes. *Process. Biochem.* **1999**, *34*, 451–465. [CrossRef]
49. Sarı, A.; Çıtak, D.; Tuzen, M. Equilibrium, thermodynamic and kinetic studies on adsorption of Sb(III) from aqueous solution using low-cost natural diatomite. *Chem. Eng. J.* **2010**, *162*, 521–527. [CrossRef]
50. Yusan, S.; Gok, C.; Erenturk, S.; Aytas, S. Adsorptive removal of thorium (IV) using calcined and flux calcined diatomite from Turkey: Evaluation of equilibrium, kinetic and thermodynamic data. *Appl. Clay Sci.* **2012**, *67-68*, 106–116. [CrossRef]
51. Tian, L.; Zhang, J.; Shi, H.; Li, N.; Ping, Q. Adsorption of Malachite Green by diatomite: Equilibrium isotherms and kinetic studies. *J. Dispers. Sci. Technol.* **2015**, *37*, 1059–1066. [CrossRef]
52. Beltrán, J.L.; Pignatello, J.J.; Teixidó, M. ISOT_Calc: A versatile tool for parameter estimation in sorption isotherms. *Comput. Geosci.* **2016**, *94*, 11–17. [CrossRef]

53. Erdem, E.; Çölgeçen, G.; Donat, R. The removal of textile dyes by diatomite earth. *J. Colloid Interface Sci.* **2005**, *282*, 314–319. [CrossRef]
54. Lin, J.X.; Wang, L. Adsorption of dyes using magnesium hydroxide-modified diatomite. *Desalination Water Treat.* **2009**, *8*, 263–271. [CrossRef]
55. Ajenifuja, E.; Ajao, J.A.; Ajayi, E.O.B. Adsorption isotherm studies of Cu (II) and Co (II) in high concentration aqueous solutions on photocatalytically modified diatomaceous ceramic adsorbents. *Appl. Water Sci.* **2017**, *7*, 3793–3801. [CrossRef]
56. Bello, O.S.; Adegoke, K.A.; Oyewole, R.O. Insights into the adsorption of heavy metals from wastewater using diatomaceous earth. *Sep. Sci. Technol.* **2014**, *49*, 1787–1806. [CrossRef]
57. Salman, T.; Temel, F.A.; Turan, N.G.; Ardali, Y. Adsorption of lead (II) ions onto diatomite from aqueous solutions: Mechanism, isotherm and kinetic studies. *Glob. Nest J.* **2016**, *18*, 1–18.
58. Dalagan, J.Q.; Ibale, R.A. Adsorption behavior of heavy metal ions (Cr^{3+}, Pb^{2+} and Cu^{2+}) into magnetite-graphite oxide-diatomite. *Asia Pac. High. Educ. Res. J.* **2016**, *3*, 114–121.
59. Pookmanee, P.; Thippraphan, P.; Phanichphant, S. Removal of heavy metals from aqueous solution by natural and modified diatomite. *J. Microsc. Soc. Thail.* **2011**, *4*, 103–107.
60. Al-Ghouti, M.; Khraisheh, M.A.M.; Ahmad, M.N.M.; Allen, S. Thermodynamic behaviour and the effect of temperature on the removal of dyes from aqueous solution using modified diatomite: A kinetic study. *J. Colloid Interf. Sci.* **2005**, *287*, 6–13. [CrossRef]
61. Zhang, J.; Ping, Q.; Niu, M.; Shi, H.; Li, N. Kinetics and equilibrium studies from the methylene blue adsorption on diatomite treated with sodium hydroxide. *Appl. Clay Sci.* **2013**, *83–84*, 12–16. [CrossRef]
62. Rusu, V.; Lupascu, T. Chemistry of sediments of aquatic systems. Surface properties. Physico-Chemical Models. Chisinau, ElenaV.I. 2004; 272p, ISBN 9975-9750-3-8. (In Romanian)